

# Thin-Layer Approximation for Three-Dimensional Supersonic Corner Flows

C. M. Hung\* and Seth S. Kurasaki†

NASA Ames Research Center, Moffett Field, Calif.

## Introduction

COMPUTATION of the three-dimensional supersonic flow over an axial corner (Fig. 1) has recently received extensive investigation.<sup>1-5</sup> As shown in Ref. 4, the computed results, using the program developed in Refs. 2 and 3, closely predict the experimental measurements of surface pressure, skin friction, and heat transfer, as well as the details of the flowfield structure for a wide range of Mach number, Reynolds number, and shock strength. All of those studies<sup>1-4</sup> were based upon the complete Navier-Stokes equations. However, in high-Reynolds-number flows, the viscous effects are confined to a region near the wall boundary and are dominated by the viscous terms associated with the strain rate in the direction normal to the wall. The viscous terms with the strain rates along the body are comparatively small and insignificant. This concept was first discussed by Prandtl in the development of boundary-layer theory and has been applied and extended to various problems. The recent development of the thin-layer approximation<sup>6</sup> is based on this concept, with the retention of unsteady and all inviscid terms of the Navier-Stokes equations. This approximation has been tested in the calculation of many flow problems,<sup>7-9</sup> and the results confirm its validity and applicability.

The purpose of this Note is to extend the thin-layer approximation to an axial corner that is formed by the intersection of two perpendicular plates, one of which has an inclination angle  $\alpha$  with respect to the freestream (Fig. 1).

## Analysis

### Thin-Layer Approximation

The computational domain is described in Ref. 3. The mesh is equally spaced in the  $x$  direction. In both  $y$  and  $z$  directions, a fine mesh spacing is used in the regions near the wall,  $0 \leq y < y_f$  and  $0 \leq z < z_f$ , to resolve the viscous effects, and coarse mesh spacing is used in the outer regions,  $y_f \leq y \leq y_h$  and  $z_f \leq z \leq z_h$ , where viscous effects are negligible. Both the fine and coarse meshes are stretched geometrically with different stretching constants.

The basic equations of the present analysis are the time-dependent compressible Navier-Stokes equations, written in conservative form

$$\frac{\partial U}{\partial t} + \frac{\partial (F - F_v)}{\partial \xi} + \frac{\partial}{\partial \eta} [G - G_v - \tan\theta (F - F_v)] + \frac{\partial (H - H_v)}{\partial \zeta} = 0 \quad (1)$$

where

$$\xi = x$$

$$\eta = y - y_b(x), \quad \tan\theta = y'_b(x) = 0 \quad \text{for } x < L$$

$$\zeta = z \quad = \tan\alpha \quad x \geq L$$

$U$  represents the conservative variables ( $\rho, \rho u, \rho v, \rho w, \rho E$ );  $F, G$ , and  $H$  are the transport inviscid fluxes; and  $F_v, G_v$ , and  $H_v$  are the corresponding transport viscous fluxes in the  $x, y$ , and  $z$  directions, respectively. Equation (1) is valid for laminar as well as for turbulent flow with the addition of a modeled eddy viscosity. In the present study, the viscous effects are dominated either by the wall at  $\eta = 0$  as  $\zeta$  becomes large, or by the wall at  $\zeta = 0$  as  $\eta$  becomes large, or by both walls near the corner region. To form the thin-layer approximation, we 1) retain all the inviscid fluxes,  $F, G$ , and  $H$ ; 2) neglect all the viscous terms associated with velocity gradients in the  $\xi$  direction; and 3) in  $\eta$  and  $\zeta$  directions, neglect all cross derivatives, while retaining second-order derivatives of  $\eta$  and  $\zeta$ ,  $\partial^2/\partial\eta^2$  in  $\partial(G_v - F_v \tan\theta)/\partial\eta$ , and  $\partial^2/\partial\zeta^2$  in  $\partial H_v/\partial\zeta$ . This results in the thin-layer approximation Navier-Stokes equations as follows:

$$\frac{\partial U}{\partial t} + \frac{\partial F}{\partial \xi} + \frac{\partial}{\partial \eta} (G - \tan\theta F - G'_v + \tan\theta F'_v) + \frac{\partial}{\partial \zeta} (H - H'_v) = 0 \quad (2)$$

where

$$G'_v = \begin{bmatrix} 0 \\ \sigma_{yx} \\ \sigma_{yy} \\ \sigma_{yz} \\ \phi_y \end{bmatrix}, \quad F'_v = \begin{bmatrix} 0 \\ \sigma_{xx} \\ \sigma_{yx} \\ \sigma_{xz} \\ \phi_x \end{bmatrix}, \quad H'_v = \begin{bmatrix} 0 \\ \sigma_{zx} \\ \sigma_{zy} \\ \sigma_{zz} \\ \phi_z \end{bmatrix}$$

$$\sigma_{xx} = \lambda \frac{\partial v'}{\partial \eta} - 2(\mu + \epsilon) \frac{\partial u}{\partial \eta} \tan\theta$$

$$\sigma_{yy} = \lambda \frac{\partial v'}{\partial \eta} + 2(\mu + \epsilon) \frac{\partial v}{\partial \eta}$$

$$\sigma_{zz} = (\lambda + 2\mu + 2\epsilon) \frac{\partial w}{\partial \zeta}$$

$$\sigma_{yx} = \mu \frac{\partial}{\partial \eta} (u - v \tan\theta)$$

$$\sigma_{yz} = \mu \frac{\partial}{\partial \eta} w, \quad \sigma_{zy} = \mu \frac{\partial v}{\partial \zeta}$$

$$\sigma_{xz} = -\mu \frac{\partial w}{\partial \eta} \tan\theta, \quad \sigma_{zx} = \mu \frac{\partial u}{\partial \zeta}$$

$$\phi_x = \sigma_{xx} u + \sigma_{yx} v + \sigma_{zx} w - \left( \frac{\gamma\mu}{Pr} + \frac{\gamma\epsilon}{Pr_t} \right) \frac{\partial e_i}{\partial \eta} \tan\theta$$

$$\phi_y = \sigma_{yx} u + \sigma_{yy} v + \sigma_{yz} w + \left( \frac{\gamma\mu}{Pr} + \frac{\gamma\epsilon}{Pr_t} \right) \frac{\partial e_i}{\partial \eta}$$

$$\phi_z = \sigma_{zx} u + \sigma_{zy} v + \sigma_{zz} w + \left( \frac{\gamma\mu}{Pr} + \frac{\gamma\epsilon}{Pr_t} \right) \frac{\partial e_i}{\partial \zeta}$$

$$v' = v - u \tan\theta$$

$$\lambda = -\frac{2}{3}(\mu + \epsilon)$$

Received Feb. 28, 1980; revision received May 22, 1980. This paper is declared a work of the U.S. Government and therefore is in the public domain.

Index categories: Computational Methods; Supersonic and Hypersonic Flow.

\*Research Scientist. Member AIAA.

†Research Engineer.

and  $\mu$  is the molecular viscosity,  $\epsilon$  the turbulent eddy viscosity,  $Pr$  the Prandtl number,  $Pr_t$  the turbulent Prandtl number,  $\gamma$  the ratio of specific heats, and  $e_i$  the internal energy. Note that  $\sigma_{yz} \neq \sigma_{zy}$  and  $\sigma_{xz} \neq \sigma_{zx}$ , and the neglected cross derivatives

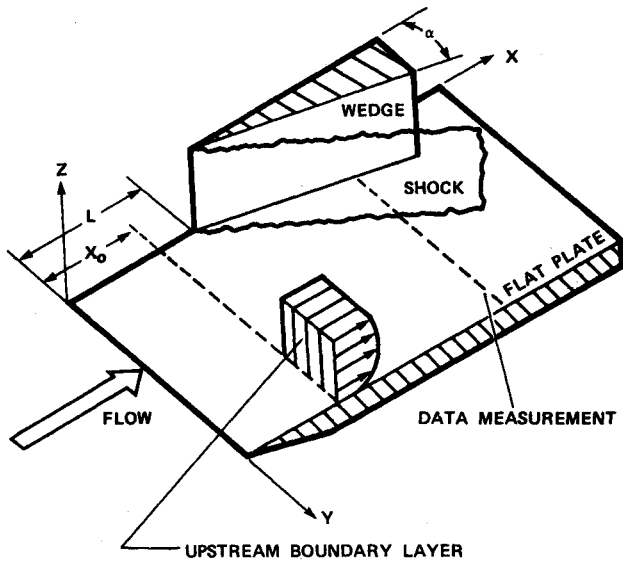


Fig. 1 Three-dimensional compression corner and swept shock wave.

can be of the same order of magnitude as the retained derivatives in  $(\partial/\partial\eta)(G'_v - F'_v \tan\theta)$  or  $(\partial/\partial\zeta)H'_v$  near the axial corner. But, while both  $\eta \rightarrow \text{small}$  and  $\zeta \rightarrow \text{small}$ , the velocity components  $v'$  and  $w$ , as well as their gradients, are small. Moreover, the flow contains comparatively very low momentum. Therefore, the neglect of cross derivatives will not significantly affect the general features of the flow.

#### Numerical Procedure

Equation (2) is then split into three groups corresponding to the coordinate directions for treatment by three operators, viz.,

$$L_\xi: \frac{\partial U}{\partial t} + \frac{\partial F}{\partial \xi} = 0$$

$$L_\eta: \frac{\partial U}{\partial t} + \frac{\partial}{\partial \eta} (G - \tan\theta F - G'_v + \tan\theta F'_v) = 0$$

$$L_\zeta: \frac{\partial U}{\partial t} + \frac{\partial}{\partial \zeta} (H - H'_v) = 0$$

The conventional two-step explicit MacCormack scheme<sup>10</sup> is used in the  $L_\xi$  operator and in the  $L_\eta$  and  $L_\zeta$  operators for their corresponding outer coarse mesh regions

$$L_\xi(0 - y_h, 0 - z_h), L_\eta(y_f - y_h, 0 - z_h), L_\zeta(0 - y_h, z_f - z_h)$$

where the arguments inside the parentheses indicate the regions in which the operators are applied. In the inner regions, the  $L_\eta$  and  $L_\zeta$  operators are split further into hyperbolic and parabolic operators for the inviscid and viscous terms, e.g.,

Hyperbolic Operators:

$$L_{\eta h}(0 - y_f, 0 - z_h): \frac{\partial U}{\partial t} + \frac{\partial}{\partial \eta} (G - \tan\theta F) = 0$$

$$L_{\zeta h}(0 - y_h, 0 - z_f): \frac{\partial U}{\partial t} + \frac{\partial}{\partial \zeta} H = 0$$

Parabolic Operators:

$$L_{\eta p}(0 - y_f, 0 - z_h): \frac{\partial U}{\partial t} + \frac{\partial}{\partial \eta} (G - \tan\theta F) = 0$$

$$L_{\zeta p}(0 - y_h, 0 - z_f): \frac{\partial U}{\partial t} + \frac{\partial}{\partial \zeta} H = 0$$

Parabolic Operators:

$$L_{\eta p}(0 - y_f, 0 - z_h): \frac{\partial U}{\partial t} - \frac{\partial}{\partial \eta} (G'_v - \tan\theta F'_v) = 0$$

$$L_{\zeta p}(0 - y_h, 0 - z_f): \frac{\partial U}{\partial t} - \frac{\partial}{\partial \zeta} H'_v = 0$$

The inviscid hyperbolic operators  $L_{\eta h}$  and  $L_{\zeta h}$  are the same as those discussed in Ref. 2. To account for the viscous terms in the inner region, the  $L_{\eta p}$  operator can be rewritten as

$$\left. \begin{aligned} \frac{\partial U'}{\partial t} - \frac{1}{\rho} \frac{\partial}{\partial \eta} \left( \nu \sec^2 \theta \frac{\partial U'}{\partial \eta} \right) &= A \\ \frac{\partial \rho}{\partial t} &= 0 \end{aligned} \right\} \quad (3)$$

where

$$U' = \begin{bmatrix} u' \\ v' \\ w \\ u'^2 \\ v'^2 \\ w^2 \\ e_i \end{bmatrix} \quad A = \begin{bmatrix} 0 \\ 0 \\ 0 \\ -2A_1 \\ -2A_2 \\ -2A_3 \\ (A_1 + A_2) \cos^2 \theta + A_3 \end{bmatrix}$$

$$u' = u + \tan\theta v$$

$$A_1 = \frac{1}{\rho} (\mu + \epsilon) \sec^2 \theta \left( \frac{\partial u'}{\partial \eta} \right)^2$$

$$A_2 = \frac{1}{\rho} (2\mu + 2\epsilon + \lambda) \sec^2 \theta \left( \frac{\partial v'}{\partial \eta} \right)^2$$

$$A_3 = \frac{1}{\rho} (\mu + \epsilon) \sec^2 \theta \left( \frac{\partial w}{\partial \eta} \right)^2$$

and  $\nu$  is a viscosity parameter equal to  $(\mu + \epsilon)$  for elements  $u', w, u'^2$ , and  $w^2$ , equal to  $(2\mu + 2\epsilon + \lambda)$  for elements  $v'$  and  $v'^2$ , and equal to  $(\gamma\mu/Pr) + (\gamma\epsilon/Pr_t)$  for the element  $e_i$ . There is a similar formula for the  $L_{\zeta p}$  operator. To solve Eq. (3), the method is the same as that discussed in Ref. 2, except here elements in the right-hand side (A) are simpler. Details of the numerical procedures, boundary conditions, and turbulent modeling are described in Refs. 2, 3, and 11.

#### Results and Remarks

The computer code developed in Ref. 3 is modified for the thin-layer approximation, and a case with Mach 5.9 and a wedge angle of 6 deg has been computed. Using the previous "asymptotic steady-state" as an initial condition, the solution is advanced another 100 time-steps for both programs (with and without the thin-layer approximation). The results from the thin-layer approximation are quite close to those from the complete Navier-Stokes equations. Table 1 gives a comparison of the present results for surface pressure and heat transfer with the Navier-Stokes solution given in Fig. 6 of Ref. 3. Good agreement is also seen in other main flowfield features such as  $u$  velocity, density, and temperature profiles

**Table 1 Surface pressure and heat transfer with and without thin-layer approximation at  $x/L = 1.763$  and  $y_s = 2.42$  cm**

Location $J$	$y/y_s$	$p/p_\infty$		$C_H \times 10^3$	
		Thin layer	$N-S$	Thin layer	$N-S$
2	0.0012	2.4508	2.4499	0.11371	0.11547
4	0.0071	2.4537	2.4528	0.34199	0.34291
6	0.0162	2.4536	2.4526	0.64163	0.64281
8	0.0303	2.4536	2.4528	0.96663	0.96823
10	0.0519	2.4484	2.4489	1.3007	1.3023
12	0.0855	2.4452	2.4457	1.7574	1.7545
14	0.1372	2.4184	2.4207	2.2502	2.2460
16	0.2170	2.3830	2.3863	2.7809	2.7594
18	0.3402	2.3026	2.3068	2.9593	2.9598
20	0.6825	1.7857	1.7890	2.2970	2.3124
22	1.0885	1.5898	1.5846	1.1604	1.1648
24	1.4945	1.4992	1.4923	0.78808	0.77688
26	1.9004	1.3079	1.3025	0.72066	0.71207
28	2.3064	1.1197	1.1182	0.84620	0.84633
30	2.7124	1.0684	1.0680	0.92207	0.92203
32	3.1183	1.0599	1.0599	0.92980	0.93131
34	3.5243	1.0582	1.0582	0.93241	0.93387

(not shown here). The good agreement is not surprising since the thin-layer approximation not only retains the most dominant terms

$$(\mu + \epsilon) \left( \frac{\partial^2 u}{\partial \eta^2} + \frac{\partial^2 u}{\partial \xi^2} \right)$$

in the streamwise momentum equation, but also retains the so-called "second-order boundary-layer terms" as derived in Ref. 12 for an incompressible flow. For this test case, the boundary layer near the corner is very thin (see Ref. 3), and the thin-layer approximation is expected to provide an accurate solution. In the present study, for 100 time-steps with a  $(21 \times 36 \times 32)$  mesh, 1266 s of computation time are required on a CDC 7600 for the thin-layer approximation, and 1524 s (20% more) for the unmodified complete Navier-Stokes solution.

In summary, this Note has demonstrated one method for extending the thin-layer approximation to an axial corner flow where the viscous effects are dominated by two perpendicular walls. In addition, it has been shown that it is not necessary to solve the complete Navier-Stokes equations for a three-dimensional, high-Reynolds-number corner flow.

## References

- <sup>1</sup>Shang, J. S. and Hankey, W. L., "Numerical Solution of Compressible Navier-Stokes Equations for a Three-Dimensional Corner," *AIAA Journal*, Vol. 15, Nov. 1977, pp. 1575-1582.
- <sup>2</sup>Hung, C. M. and McCormack, R. W., "Numerical Solution of Supersonic Laminar Flow over a Three-Dimensional Compression Corner," *AIAA Paper 77-694*, Albuquerque, N. Mex., June 1977.
- <sup>3</sup>Hung, C. M. and McCormack, R. W., "Numerical Solution of Three-Dimensional Shock Wave and Turbulent Boundary-Layer Interaction," *AIAA Journal*, Vol. 16, Oct. 1978, pp. 1090-1096.
- <sup>4</sup>Horstman, C. C. and Hung, C. M., "Computation of Three-Dimensional Turbulent Separated Flows at Supersonic Speeds," *AIAA Journal*, Vol. 17, Nov. 1979, pp. 1155-1156.
- <sup>5</sup>Shang, J. S., Hankey, W. L., and Petty, J. S., "Three-Dimensional Supersonic Interacting Turbulent Flow along a Corner," *AIAA Journal*, Vol. 17, July 1979, pp. 706-713.
- <sup>6</sup>Baldwin, B. S. and Lomax, H., "Thin-Layer Approximation and Algebraic Model for Separated Turbulent Flow," *AIAA Paper 78-257*, Huntsville, Ala., Jan. 1978.
- <sup>7</sup>Pulliam, T. H. and Steger, J. L., "Implicit Finite-Difference Simulation of Three-Dimensional Compressible Flow," *AIAA Journal*, Vol. 18, Feb. 1980, pp. 159-167.
- <sup>8</sup>Hung, C. M., "Numerical Solution of Supersonic Laminar Flow over an Inclined Body of Revolution," *AIAA Journal*, Vol. 18, Aug. 1980, pp. 921-928.
- <sup>9</sup>Schiff, L. B. and Sturek, W. B., "Numerical Simulation of Steady Supersonic Flow over an Ogive-Cylinder-Boattail Body," *AIAA Paper 80-0066*, Pasadena, Calif., Jan. 1980.
- <sup>10</sup>McCormack, R. W. and Baldwin, B. S., "A Numerical Method for Solving the Navier-Stokes Equations with Application to Shock Boundary-Layer Interactions," *AIAA Paper 75-1*, Pasadena, Calif., Jan. 1975.
- <sup>11</sup>McCormack, R. S., "An Efficient Numerical Method for Solving the Time-Dependent Compressible Navier-Stokes Equations at High Reynolds Number," *NASA TM X-73,129*, July 1976.
- <sup>12</sup>Rubin, S. G., "Incompressible Flow along a Corner," *Journal of Fluid Mechanics*, Vol. 26, Pt. 1, Sept. 1966, pp. 97-110.